Article

Picosecond Photoreduction of Inducible Nitric Oxide Synthase by Rhenium(I)–Diimine Wires

Wendy Belliston-Bittner, Alexander R. Dunn, Yen Hoang Le Nguyen, Dennis J. Stuehr, Jay R. Winkler, and Harry B. Gray

J. Am. Chem. Soc., **2005**, 127 (45), 15907-15915• DOI: 10.1021/ja0543088 • Publication Date (Web): 19 October 2005

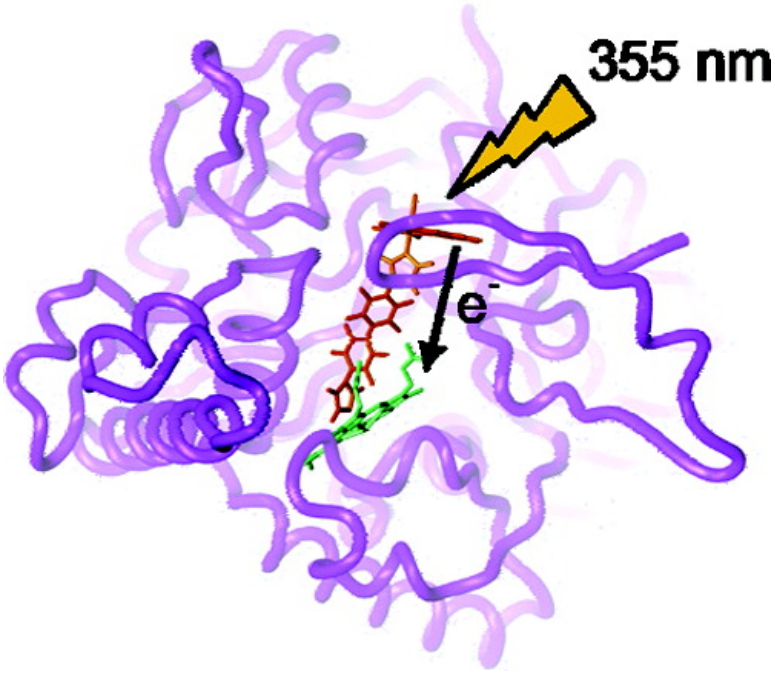

More About This Article

Additional resources and features associated with this article are available within the HTML version:

- Supporting Information
- Links to the 9 articles that cite this article, as of the time of this article download
- Access to high resolution figures
- Links to articles and content related to this article
- Copyright permission to reproduce figures and/or text from this article

J|A|C|S
ARTICLES
Published on Web 10/19/2005

Picosecond Photoreduction of Inducible Nitric Oxide Synthase by Rhenium(I)−Diimine Wires

Wendy Belliston-Bittner,[†] Alexander R. Dunn,[†,‡] Yen Hoang Le Nguyen,[†] Dennis J. Stuehr,[§] Jay R. Winkler,[†] and Harry B. Gray*,[†]

Contribution from the Beckman Institute, California Institute of Technology, Pasadena, California 91125, Department of Biochemistry, Stanford University, Stanford, California 94305, and Department of Immunology, Lerner Research Institute, The Cleveland Clinic, Cleveland, Ohio 44195

Received June 29, 2005; E-mail: hbgray@caltech.edu

Abstract: In a continuing effort to unravel mechanistic questions associated with metalloenzymes, we are developing methods for rapid delivery of electrons to deeply buried active sites. Herein, we report picosecond reduction of the heme active site of inducible nitric oxide synthase bound to a series of rhenium−diimine electron-tunneling wires, $[Re(CO)_3LL']^+$, where L is 4,7-dimethylphenanthroline and L′ is a perfluorinated biphenyl bridge connecting a rhenium-ligated imidazole or aminopropylimidazole to a distal imidazole (F_8bp-im (**1**) and C_3-F_8bp-im (**2**)) or F (F_9bp (**3**) and C_3-F_9bp (**4**)). All four wires bind tightly (K_d in the micromolar to nanomolar range) to the tetrahydrobiopterin-free oxidase domain of inducible nitric oxide synthase (iNOSoxy). The two fluorine-terminated wires displace water from the active site, and the two imidazole-terminated wires ligate the heme iron. Upon 355-nm excitation of iNOSoxy conjugates with **1** and **2**, the active site Fe(III) is reduced to Fe(II) within 300 ps, almost 10 orders of magnitude faster than the naturally occurring reduction.

Introduction

Nitric oxide synthase (NOS) is a P450-type iron−heme enzyme that catalyzes the synthesis of nitric oxide (•NO) and L-citrulline from L-arginine and O_2.[1] There are at least three types of NOS expressed by mammals: neuronal NOS (nNOS), endothelial NOS (eNOS), and inducible NOS (iNOS). iNOS is expressed transiently in a variety of cells as a response to immunostimulation.[2] Owing mainly to the role •NO plays as a signaling molecule in an astonishing number of bodily processes, NOS malfunction is implicated in a wide array of diseases.[3−7] Specifically, •NO overproduction by iNOS is involved directly in the pathology of inflammation in diseases such as rheumatoid arthritis, septic shock, atherosclerosis, and diabetes.[2,7] These findings have brought NOS and its catalytic mechanism into the spotlight as targets of great pharmacological interest.

All three mammalian NOS enzymes exist in vivo as homodimers, with each monomer consisting of a C-terminal reductase module, an intervening calmodulin-binding domain, and an N-terminal oxidase domain.[8,9] The reductase module of one subunit provides reducing equivalents to the catalytically active, heme-containing oxidase domain of the other subunit.[10] NOS turns over twice en route to •NO production. The mechanism of the first turnover (from L-arginine to *N*-hydroxy-L-arginine) is expected to be similar to that of P450, while the second turnover is believed to proceed differently (Scheme 1).[8,9,11−13] The first steps of each oxygenation are well-characterized and include reduction of the heme followed by O_2 binding and a second reduction.[12,14,15] Because of the sluggishness of the second electron transfer ($\sim 12\ s^{-1}$),[12,14,15] and the speed of subsequent reaction(s), very little is known about the active intermediates.[13,16,17]

One goal of our research program is to use photoactive wires to trigger the second electron transfer to the NOS heme in an

[†] California Institute of Technology.
[‡] Stanford University.
[§] The Cleveland Clinic.

(1) Stuehr, D. J. *Biochim. Biophys. Acta−Bioenergetics* **1999**, *1411*, 217−230.
(2) Aktan, F. *Life Sci.* **2004**, *75*, 639−653.
(3) Luth, H. J.; Holzer, M.; Gertz, H. J.; Arendt, T. *Brain Res.* **2000**, *852*, 45−55.
(4) Luth, H. J.; Holzer, M.; Gartner, U.; Staufenbiel, M.; Arendt, T. *Brain Res.* **2001**, *913*, 57−67.
(5) Kendrick, K. M.; Guevara-Guzman, R.; Zorrilla, J.; Hinton, M. R.; Broad, K. D.; Mimmack, M.; Ohkura, S. *Nature* **1997**, *388*, 670−674.
(6) Huang, P. L.; Huang, Z. H.; Mashimo, H.; Bloch, K. D.; Moskowitz, M. A.; Bevan, J. A.; Fishman, M. C. *Nature* **1995**, *377*, 239−242.
(7) Hingorani, A. D.; Cross, J.; Kharbanda, R. K.; Mullen, M. J.; Bhagat, K.; Taylor, M.; Donald, A. E.; Palacios, M.; Griffin, G. E.; Deanfield, J. E.; MacAllister, R. J.; Vallance, P. *Circulation* **2000**, *102*, 994−999.
(8) Groves, J. T.; Wang, C. C. Y. *Curr. Opin. Chem. Biol.* **2000**, *4*, 687−695.
(9) Alderton, W. K.; Cooper, C. E.; Knowles, R. G. *Biochem. J.* **2001**, *357*, 593−615.
(10) Crane, B. R.; Rosenfeld, R. J.; Arvai, A. S.; Ghosh, D. K.; Ghosh, S.; Tainer, J. A.; Stuehr, D. J.; Getzoff, E. D. *EMBO J.* **1999**, *18*, 6271−6281.
(11) Wei, C. C.; Crane, B. R.; Stuehr, D. J. *Chem. Rev.* **2003**, *103*, 2365−2383.
(12) Stuehr, D. J.; Santolini, J.; Wang, Z. Q.; Wei, C. C.; Adak, S. *J. Biol. Chem.* **2004**, *279*, 36167−36170.
(13) Davydov, R.; Ledbetter-Rogers, A.; Martasek, P.; Larukhin, M.; Sono, M.; Dawson, J. H.; Masters, B. S. S.; Hoffman, B. M. *Biochemistry* **2002**, *41*, 10375−10381.
(14) Wei, C. C.; Wang, Z. Q.; Hemann, C.; Hille, R.; Stuehr, D. J. *J. Biol. Chem.* **2003**, *278*, 46668−46673.
(15) Wei, C. C.; Wang, Z. Q.; Arvai, A. S.; Hemann, C.; Hille, R.; Getzoff, E. D.; Stuehr, D. J. *Biochemistry* **2003**, *42*, 1969−1977.
(16) Bec, N.; Gorren, A. C. F.; Voelker, C.; Mayer, B.; Lange, R. *J. Biol. Chem.* **1998**, *273*, 13502−13508.

Scheme 1. Proposed Mechanisms for the First and Second Turnovers of NOS[9,12,13,18,a]

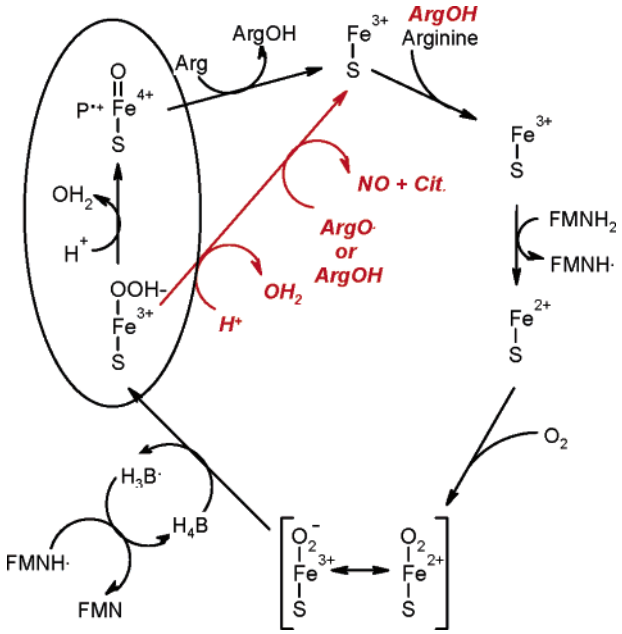

[a] Known and hypothetical differences between the first and second turnovers are noted in red. Putative intermediates of particular interest are in the upper left ellipse.

attempt to observe high-valent intermediates directly. In recent work, we took the first step toward this goal by building ruthenium and rhenium wires (Re wires **1** and **3**, Chart 1) that bind tightly to the monomeric oxidase domain of iNOS (iNOSoxy).[19] These wires and analogues **2** and **4** (Chart 1) are based on complexes that have been shown previously to bind to and rapidly reduce P450cam upon photoexcitation.[20−22] Strikingly, two of the bound wires, **1** and **2**, photoreduce iNOSoxy in less than 300 ps, nearly 10 orders of magnitude faster than the natural reduction.[23]

Results

Synthesis and Characterization of Wires. Nucleophilic substitution on decafluorobiphenyl proceeds readily (Scheme 2). Addition of two equivalents of nucleophile to decafluorobiphenyl will produce the doubly substituted product (such as **7** in Scheme 2) in approximately 100% yield. In our hands, addition of fewer than two equivalents of nucleophile always produces a mixture of singly and doubly substituted products. These mixtures were easily separated by flash chromatography or sublimation.

Chart 1. Re Wires That Bind iNOSoxy[a]

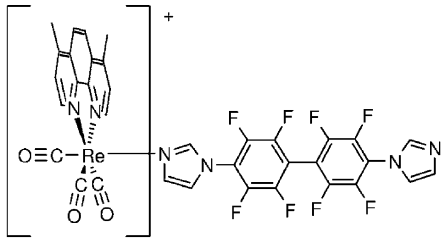

1 = Re-Im-F_8bp-Im

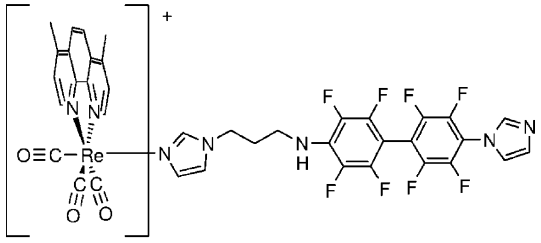

2 = Re-Im-C_3-F_8 bp-Im

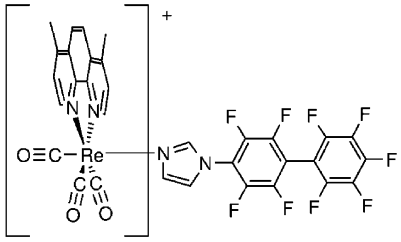

3 = Re-Im-F_9bp

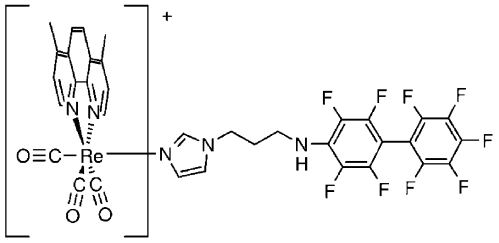

4 = Re-Im-C_3-F_9bp

[a] Excitation of bound **1** or **2** triggers reduction of the enzyme within 300 ps.

Ligation of imidazole-based complexes **6**, **7**, and **8** to rhenium is a slow and inefficient reaction. Attempts to speed up the reaction by heating above 40 °C generally caused a decrease in yield. In some samples, the BF_4^- counterion was exchanged for trifluoromethanesulfonate (triflate, OTf^-) due to observations that the triflate salts were easier to purify. There were no measurable differences in the solubility, protein binding, or photophysical properties of the triflate and BF_4^- salts.

Typical of Re−diimines, all four complexes have very similar spectroscopic behavior, with metal-to-ligand charge-transfer absorption bands centered at ∼320 and 360 nm, emission maxima at 560 nm, and microsecond luminescence lifetimes (Table 1). All four wires have 4−5% luminescence quantum yields in water, and **1** and **3** have Förster distances (R_0) of 32 ± 8 Å in the presence of Δ65 iNOSoxy.[24]

(17) In 1998, Bec et al.[16] reported a low-temperature optical spectrum of a complex they hypothesized to be compound I (ferryl heme). While this paper has since been heavily cited, the lack of reference to this particular spectrum and the lack of subsequent reproduction of this species calls their assignment into question. Additionally, in 2002, Davydov et al.[13] reported EPR and ENDOR characterization of a peroxy heme intermediate at cryogenic temperatures. These were the first and, to our knowledge, only reported spectroscopic characterizations of post-oxyferrous heme-based intermediates in NOS.

(18) Werner, E. R.; Gorren, A. C. F.; Heller, R.; Werner-Felmayer, G.; Mayer, B. *Exp. Biol. Med.* **2003**, *228*, 1291−1302.
(19) Dunn, A. R.; Belliston-Bittner, W.; Winkler, J. R.; Getzoff, E. D.; Stuehr, D. J.; Gray, H. B. *J. Am. Chem. Soc.* **2005**, *127*, 5169−5173.
(20) Wilker, J. J.; Dmochowski, I. J.; Dawson, J. H.; Winkler, J. R.; Gray, H. B. *Angew. Chem., Int. Ed.* **1999**, *38*, 89−92.
(21) Dunn, A. R.; Dmochowski, I. J.; Winkler, J. R.; Gray, H. B. *J. Am. Chem. Soc.* **2003**, *125*, 12450−12456.
(22) Dmochowski, I. J.; Crane, B. R.; Wilker, J. J.; Winkler, J. R.; Gray, H. B. *Proc. Natl. Acad. Sci. U.S.A.* **1999**, *96*, 12987−12990.
(23) Presta, A.; Siddhanta, U.; Wu, C. Q.; Sennequier, N.; Huang, L. X.; Abu-Soud, H. M.; Erzurum, S.; Stuehr, D. J. *Biochemistry* **1998**, *37*, 298−310.

Scheme 2. Synthesis of Re−Diimine Wires

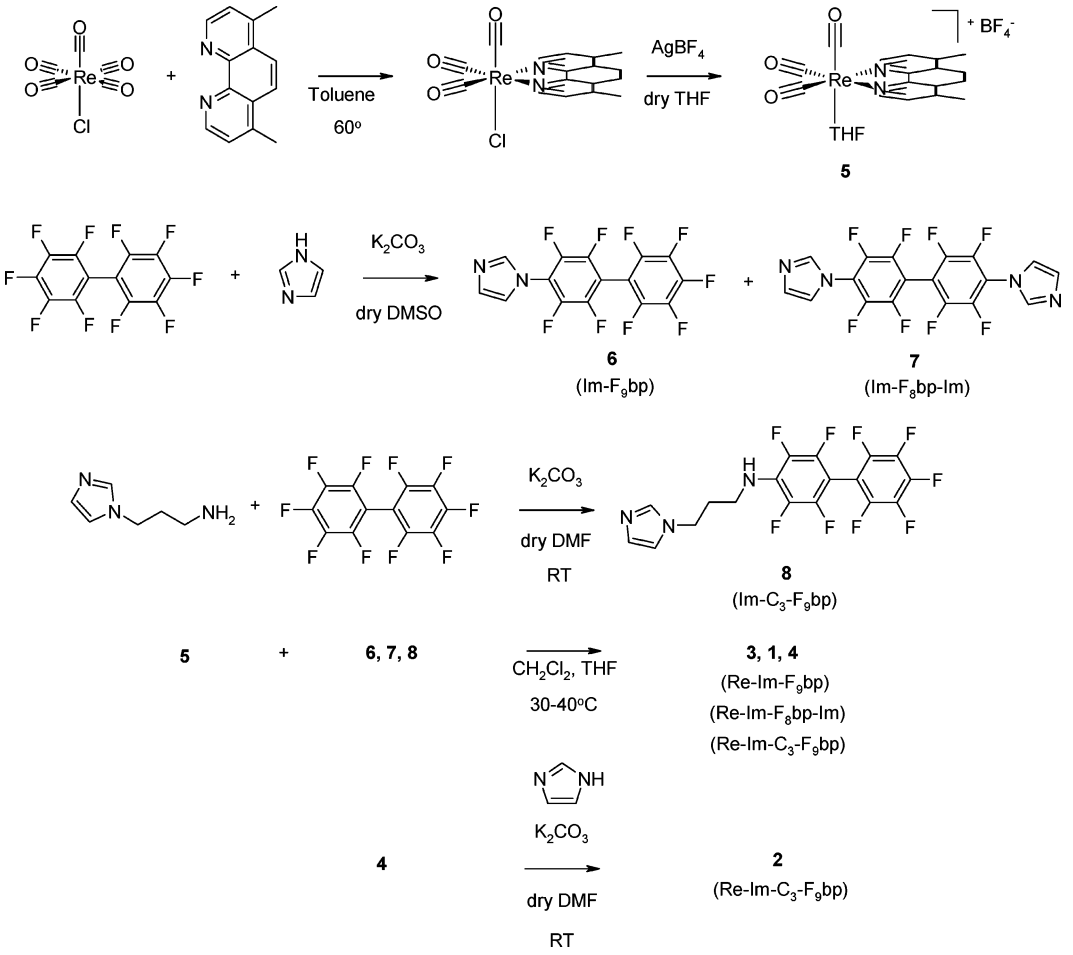

Table 1. Re Wire Characterization and Dissociation Constants in Conjugates with Δ65 iNOSoxy[a]

wire	ϵ_{360} ($mM^{-1}\,cm^{-1}$)	τ_L (μs)	ϕ	R_0 (Å)	K_d with Δ65 (μM)
1	4.1(4)	0.97(3)	0.055(2)	32(8)	0.13(7)
2[b]	5.0(4)	0.78(1)	0.04(1)[c]		<10
3	4.1(6)	0.95(4)	0.054(1)	32(8)	1.4(5)
4[b]	4.3(4)	0.79(1)	0.042(6)[c]		<10

[a] Except where noted, numbers in parentheses are standard deviations based on at least three separate measurements. [b] Measured in 50% glycerol. [c] Average of two measurements.

Wire Binding to Δ65 iNOS. All four complexes described above bind in the active-site channel of Δ65 iNOSoxy. Imidazole-terminated wires **1** and **2** ligate the heme iron, causing a characteristic red shift in the Soret band. Fluorophenyl-terminated complexes **3** and **4** displace water from the active site, causing a partial (blue) shift toward high-spin Fe(III) (Figure 1).

The **3**:Δ65 conjugate has a dissociation constant of 1.4 ± 0.5 μM, as determined by measurements of luminescence decay kinetics (Figure 2A). These data are similar to those previously described for the **3**:Δ114 iNOSoxy complex, suggesting Förster energy-transfer quenching of the Re excited state and a Re−heme distance of ∼18 Å.[19]

Luminescence decay measurements on a 1:1 mixture of Δ65 and imidazole-terminated wire **1** (Figure 2B) show that Re(I)* lifetime in the bound wire is much less than 10 ns.[25] Furthermore, there is no apparent free wire in solution (as evidenced by the lack of a long-lived species). A dissociation constant for the complex could not, therefore, be calculated from the transient luminescence data. Instead, a dissociation constant of 130 ± 70 nM was calculated from steady-state luminescence measurements of **1** alone and in the **1**:Δ65 complex (Figure 3).[19]

Owing to low solubility and a tendency to aggregate in water, the concentrations of wires **2** and **4** in buffer could not be

(24) The 25% error in these calculations occurs due to the assumptions that κ^2 is equal to 2/3. The danger in setting $\kappa^2 = 2/3$ is that the rhenium and heme species are not likely to be freely rotating with respect to one another in this bound system. This restricted motion is less of a problem for calculating similar values for $Ru(bpy)_3^{2+}$-based wires due to the existence of three perpendicular transition dipoles for the octahedral $Ru(bpy)_3^{2+}$ species. The rhenium species being studied here, however, has a unidirectional transition dipole in the plane of the phenanthroline ligand. This suggests that assuming $\kappa^2 = 2/3$ could cause a large error in the calculated R_0 value. The largest error would occur if the rhenium transition dipole was oriented exactly perpendicular to that of the heme. In this case, κ^2 would be 0, and no FET would occur. Because quenching has been observed, this extreme case is unlikely. Otherwise, because the sixth root is taken to determine R_0, κ^2 values ranging from 1 to 4 produce up to a 25% error in the calculation. Crystal structures of the wire−NOS complexes and anisotropy measurements will help to sort out this problem in the future. Given the current limited understanding of the orientation of the rhenium with respect to the heme in this system, the maximal 25% error was assumed. Some error could also come from assuming that $n = 1.34$ (the refractive index of water). While studies were conducted in buffer solution, the environment of the donor and acceptor is the protein channel. Because the error due to the κ^2 factor is likely to be much greater, however, the error in n was not accounted for in these calculations.

(25) Several attempts were made to measure the luminescence lifetimes of the bound wires using the faster instrument on which the psTA measurements were taken. These attempts were unsuccessful, however, due to the fact that the protein itself is luminescent with a lifetime of approximately 200 ps when excited at 355 nm. The origin of this luminescence remains unknown, but it dominates the decay kinetics in wire:protein mixtures to the point that decay constants for the bound wires cannot be extracted. They are, therefore, reported here as less than or equal to 200 ps.

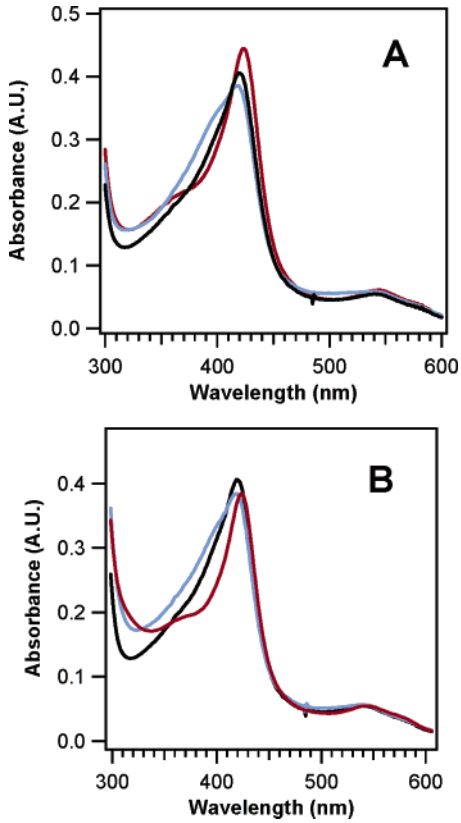

Figure 1. UV−visible absorption spectra of Δ65:wire complexes. (A) Δ65 alone (5 μM; black) and bound to 1 equiv each of **1** (Re-Im-F_8bp-Im; red) and **3** (Re-Im-F_9bp; blue). (B) Δ65 alone (5 μM; black) and bound to approximately 1 equiv each of **2** (Re-Im-C_3-F_8bp-Im; red) and **4** (Re-Im-C_3-F_9bp; blue).

measured precisely, so the micromolar dissociation constants for both wires conjugated with Δ65 were estimated from UV−vis spectra (Figure 1B) and luminescence decay kinetics (Figure 2C,D). Addition of approximately one equivalent of each wire to micromolar solutions of Δ65 produced Soret band shifts similar to those observed with the shorter, more soluble wires **1** and **3**. Luminescence decay kinetics also indicated an appreciable proportion of bound, quenched wire in each case. In the protein:wire mixtures, the wires show an extremely fast phase (below the instrument response time), corresponding to bound wire, and two slower phases arising from free and aggregated wire. The signal attributable to unbound wire was similar to that observed for the protein:**3** mixture, suggesting that these wires likely bind about as tightly as **3**.

Electron Transfer. Transient absorbance measurements show that, upon 355 nm excitation, imidazole-terminated wires **1** and **2** reduce iNOS (Figure 4 and Supporting Information). Reduction is indicated by a bleach centered near 420 nm (the disappearance of six-coordinate Fe(III)) and an optical density increase centered around 445 nm (the appearance of six-coordinate Fe(II)). Difference spectra were constructed from single-wavelength transient absorbance traces 80 ns after excitation of the **2**:Δ65 complex (Figure 5, blue) and 3 μs after excitation of the **1**:Δ65 complex (Figure 5, red). These spectra bear a striking resemblance to that previously reported for photoreduction of *N*-phenylimidazole-ligated P450cam, another heme−thiolate enzyme.[21]

With both wire complexes, the photoproduced Fe(II) signal shows multiexponential decay kinetics that consist of three dominant phases, $k_{b1} = 6(1) \times 10^6\ s^{-1}$, $k_{b2} = 2.5(4) \times 10^5\ s^{-1}$, and $k_{b3} = 6(1) \times 10^4\ s^{-1}$ (Figure 4). Using $\Delta\epsilon_{445} = 59.6\ mM^{-1}\ cm^{-1}$ (see the Experimental Section), the calculated average quantum yield of ferrous heme for both wires is 8 ± 2%. The findings that the Fe(II) absorbance maximum does not shift from 445 nm up to 250 μs confirms that the wire does not dissociate from the heme upon excitation.

Picosecond transient absorption measurements demonstrated rapid formation of Fe(II) in the presence of wires **1** and **2**. By pumping with 70-ps, 355-nm pulses and probing with 442-nm radiation from a continuous-wave He:Cd laser, we were able to obtain transient absorbance traces that show the formation of the ferrous heme at very short times (Figure 6 and Supporting Information). The traces were fit to one exponential (eq 1) to give $k_f = 7(3) \times 10^9\ s^{-1}$ for formation of Fe(II). The lack of a signal in the protein:**4** trace confirms that the observed absorbance is attributable to Fe(II) and not to Re(I)* (Supporting Information).

Discussion

Synthesis. Wires **1** and **3** were synthesized concomitantly. Their design was based on those of Ru-bpy-based wires that bind tightly to P450cam.[20−22] In prior work, substituted perfluorobiphenyls were shown not only to be synthetically versatile but also to be very efficient bridges for electron transfer. Further investigation also has suggested that their hydrophobicity and potential ability to π-stack facilitate binding to target proteins, even when a bulky sensitizer prevents them from binding in an active-site channel.[19,21]

The purpose of switching to a rhenium-based species was two-fold: to take advantage of the smaller *fac*-tricarbonylrhenium(I) phenanthryl sensitizer in comparison with the bulkier $Ru(bpy)_3^{2+}$ complex,[19] and to increase the luminescence lifetime (1 μs vs 200 ns) of the sensitizer in order to have a better chance to quench reductively.

Luminescence Quenching and Electron Transfer. In the case of **3**, quenching of the bound wire is consistent with Förster energy transfer from electronically excited rhenium to the heme roughly 18 Å away. These data support a model in which the wire is wedged far enough down the active-site channel for its terminal fluorine to displace water from the sixth coordination site on the iron (see Figure 7). This conclusion is further supported by UV−visible absorption data that show the heme spectrum shifting toward that of a five-coordinate, high-spin structure (Figure 1A).

In the case of the other three wires, luminescence quenching is too rapid (≤200 ps)[25] to be explained by Förster energy transfer. Because of the rigidity of the perfluorobiphenyl moiety, no sensible binding model can be created in which the terminal imidazole or fluorine can come near the heme while allowing the rhenium sensitizer to approach closely enough to be quenched by energy transfer in less than 200 ps. Some other mechanism surely must be operative. The production of Fe(II) confirms that electron transfer must be involved in the luminescence quenching of **1** and **2**.

In follow-up experiments, the rate of formation of Fe(II) after excitation of the samples was measured. Interference by stray fluorescence from the protein was eliminated by placing the sample far from the detector and using a laser rather than a flash lamp to probe the absorbance before and after excitation. The resulting traces (Figure 6 and Supporting Information)

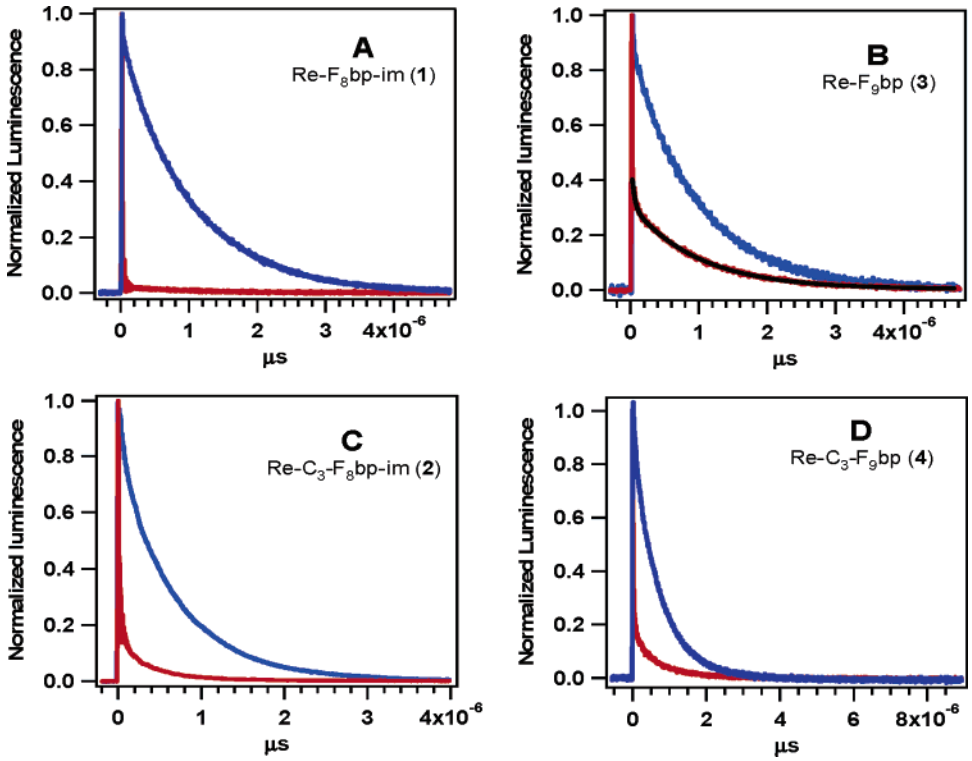

Figure 2. Transient luminescence decays of wires in solution and bound to Δ65 iNOSoxy. (A) **1** (blue) and a 1:1 mixture of **1** and Δ65 (11 μM; red). The lack of an apparent slow decay indicates that almost all of the wire is bound to the enzyme. (B) **3** (blue) and a 1:1 mixture of **3** and Δ65 (7 μM; red) and biexponential fit ($k_L = 8(1) \times 10^6$ s^{-1}, $k_0 = 1.0(3) \times 10^6$ s^{-1}, black). The fast component of the luminescence decay (k_L) corresponds to **3** bound to Δ65. (C) **2** (blue) and a 1:1 mixture of **2** and Δ65 (5 μM; red). (D) **4** (blue) and a 1:1 mixture of **4** and Δ65 (2 μM; red). In both C and D, the fastest component of the luminescence decay, corresponding to **2** or **4** bound to Δ65, is unresolvable on this time scale. The slower, visible, biexponential decay matches the biexponential decay of the wire alone in water solution (blue trace) and likely corresponds to a mixture of free and aggregated wire (fits are shown in Supporting Information).

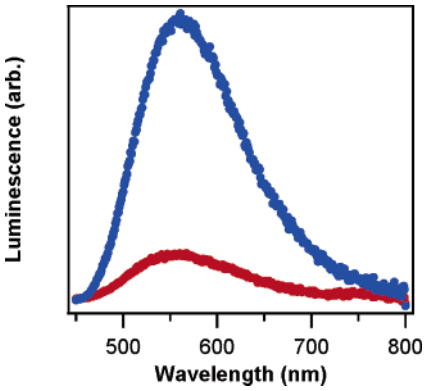

Figure 3. Steady-state fluorescence spectra of **1** (2 μM; blue) and a 1:1 mixture of **1** and Δ65 (2 μM; red) with $\lambda_{ex} = 355$ nm.

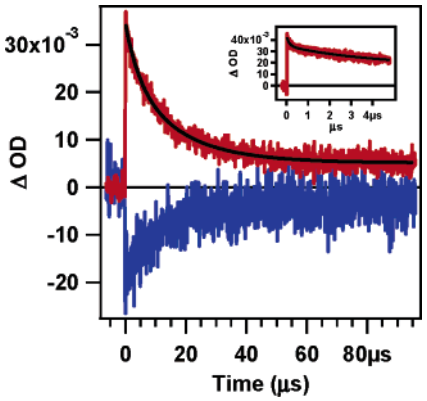

Figure 4. Transient absorbance of a 1:1 mixture of **1** and Δ65 (11 μM) showing the prompt formation and initial decay of a six-coordinate, ferrous heme. $\lambda_{ex} = 355$ nm, $\lambda_{obs} = 445$ nm (red), $\lambda_{obs} = 420$ nm (blue), biexponential fit ($k_{b2} = 2.1(1) \times 10^5$ s^{-1}, $k_{b3} = 6(1) \times 10^4$ s^{-1}, black). Inset shows the data at 445 nm taken on a shorter time scale (red) fit to two exponentials ($k_{b1} = 6(1) \times 10^6$ s^{-1}, $k_{b2} = 2.5(4) \times 10^5$ s^{-1}, black). Taken together, these traces show that the Fe(II) signal has a complicated decay pathway that requires at least three exponentials to be fit adequately.

demonstrate ferrous heme formation with a time constant less than 300 ps with wires **1** and **2** bound and additionally confirm the absence of an Fe(II) signal with wire **4** bound. This remarkably rapid photoreduction occurs almost 10 orders of magnitude faster than the initial reduction of NOS by its reductase module.[12]

Mechanistic Considerations. The observed picosecond reduction of the NOS heme by **1** and **2** is well outside the time/distance range established for single-step electron tunneling through a protein medium.[27] How can an electron make its way from a photoexcited rhenium to a heme approximately 20 Å distant with such incredible speed? Based on related work with cytochrome P450cam,[21] our original thought was that the rapid luminescence quenching was due to direct electron transfer (ET) from photoexcited rhenium to the heme. The initial nanosecond transient absorbance experiments with fully conjugated wire **1**, showing a prompt Fe(II) signal (Figure 4), appeared to support this interpretation.

(26) Crane, B. R.; et al. *Science* **1998**, *279*, 2121−2126.

(27) Gray, H. B.; Winkler, J. R. *Proc. Natl. Acad. Sci. U.S.A.* **2005**, *102*, 3534−3539.

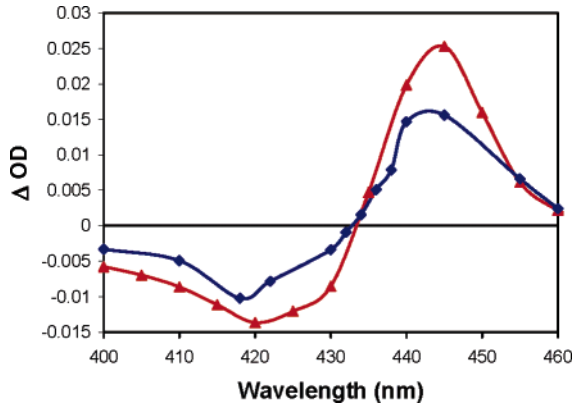

Figure 5. Difference spectra of a 1:1 mixture of **2** and Δ65 (5 μM, 80 ns after 355-nm excitation, blue squares) and a 1:1 mixture of **1** and Δ65 (11 μM, 3 μs after 355-nm excitation, red triangles) showing a bleach of a six-coordinate Fe(III) Soret (420 nm) and the appearance of a six-coordinate Fe(II) Soret (445 nm). Individual points were taken from single-wavelength transient absorbance traces.

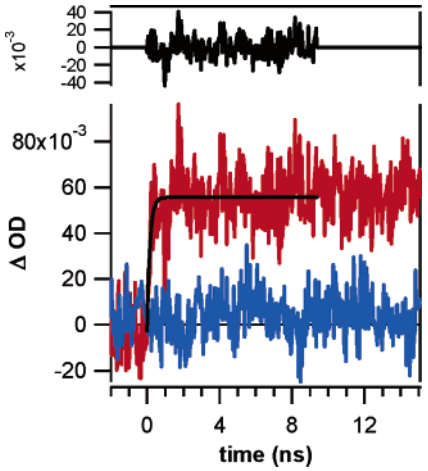

Figure 6. Transient absorbance at 442 nm of Δ65 iNOSoxy alone (8 μM, blue) and in the presence of excess **1** (red) with λ_{ex} = 355 nm. The red trace shows the rapid formation of ferrous heme fit to one exponential (k_f = 7(3) × 10^9 s^{-1}, black) with the residual shown above.

Wires **2** and **4** were, therefore, designed to test this model. The addition of a three-carbon linker between the sensitizer and the heme should have slowed photoinduced ET, both by increasing the Re−Fe distance and by disrupting the conjugation in the bridging unit. Additionally, the extended Re−Fe distance should have increased the luminescence lifetime of the Re sensitizer in **4**, the longer analogue of wire **3**. Both new wires, however, showed the same, dramatically fast luminescence quenching that had been seen with wire **1**. With wire **4**, this was true even though there was no Fe(II) signal observed. Additionally, measurement of the rate of formation of Fe(II) showed that heme reduction by wire **2** was as rapid as that observed with wire **1** (Figure 6 and Supporting Information). Finally, Fe(II) formation itself is simply too fast to be explained by this model. The $Re^{II/I}$* couple has approximately the same reduction potential as the $Ru^{III/II}$* couple in $Ru(tmbpy)_3$, the six-coordinate heme $Fe^{III/II}$ potentials for iNOSoxy and P450cam are not very different (Table 2), and the bridging units between sensitizer and heme for **1** and the Ru wires we reported[21] are virtually identical, leaving few possibilities to account for the >100-fold faster heme reduction by the Re wires. Even if activationless tunneling through a bridge as strongly coupled as poly-xylyl is invoked, the observed ET reaction is still orders of magnitude faster than expected.[27]

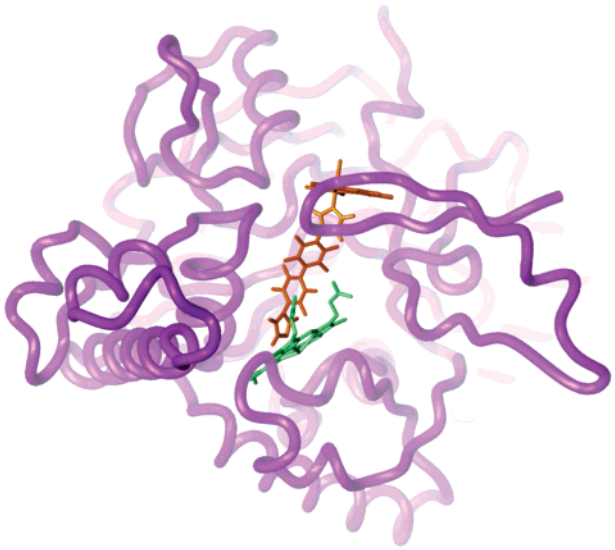

Figure 7. Model of wire **1** bound to Δ65 iNOSoxy. The wire is shown in orange, the protein backbone in purple, and the heme cofactor in green. The modeled Re−Fe distance is 18 Å. The model was created using Insight II from a crystal structure of pterin-bound, fully dimeric NOS[26] that likely has a more closed channel than is present in pterin-free iNOSoxy. The rigidity of the wire and our finding that the distal imidazole ligates the heme suggest, however, that the rhenium−heme distance should be fairly independent of the channel conformation. The other three wires are expected to bind in similar fashion.

Table 2. Reduction Potentials

redox couple	potential (V vs NHE)
$[Re(CO)_3(phen)(im)]^{II/I*}$	−0.7[a]
$[Re(CO)_3(phen)(im)]^{I*/0}$	~1.5[a]
$TrpH^{\bullet+}$/TrpH	1.15[b]
$[Ru(tmbpy)_3]^{III/II*}$	−0.75[c]
low-spin iNOSoxy ($Fe^{III/II}$)	−0.35[d]
low-spin P450cam ($Fe^{III/II}$)	~ −0.3[e]

[a] Reference 28. [b] Reference 29. [c] Reference 30. [d] Reference 31. [e] References 32 and 33.

Electronically excited $[Re(CO)_3(phen)(im)]^+$ is a powerful oxidant; indeed, Re(I)* can oxidize tryptophan (Table 2).[34] In the model of wire **1** bound to Δ65 iNOSoxy (Figure 7), two tryptophan residues, Trp_{490} and Trp_{73}, lie near the mouth of the active-site channel and in close proximity to the modeled wire. We propose that one of these tryptophan residues reductively quenches (4,7-dmp)Re(I)* to generate $TrpH^{\bullet+}$ and "Re(0)". Because Trp_{73} is missing in Δ114 iNOSoxy, in which the same rapid quenching of the wire **1** had earlier been observed,[19] the most likely candidate for reduction of Re(I)* is Trp_{490} (highlighted in blue in Figure 8).

On the basis of the structural model shown in Figure 8, we propose the quenching and electron-transfer mechanisms out-

(28) Connick, W. B.; Di Bilio, A. J.; Hill, M. G.; Winkler, J. R.; Gray, H. B. *Inorg. Chim. Acta* **1995**, *240*, 169−173.
(29) Harriman, A. *J. Phys. Chem.* **1987**, *91*, 6102−6104.
(30) Elliott, C. M.; Freitag, R. A.; Blaney, D. D. *J. Am. Chem. Soc.* **1985**, *107*, 4647−4655.
(31) Presta, A.; Weber-Main, A. M.; Stankovich, M. T.; Stuehr, D. J. *J. Am. Chem. Soc.* **1998**, *120*, 9460−9465.
(32) Sligar, S. G.; Gunsalus, I. C. *Proc. Natl. Acad. Sci. U.S.A.* **1976**, *73*, 1078−1082.
(33) Gunsalus, I. C.; Meeks, J. R.; Lipscomb, J. D. *Ann. N.Y. Acad. Sci.* **1973**, *212*, 107−121.
(34) Miller, J. E.; Grodinaru, C.; Di Bilio, A. J.; Wehbi, W. A.; Crane, B. R.; Winkler, J. R.; Gray, H. B. *J. Am. Chem. Soc.* **2003**, *125*, 14220−14221.

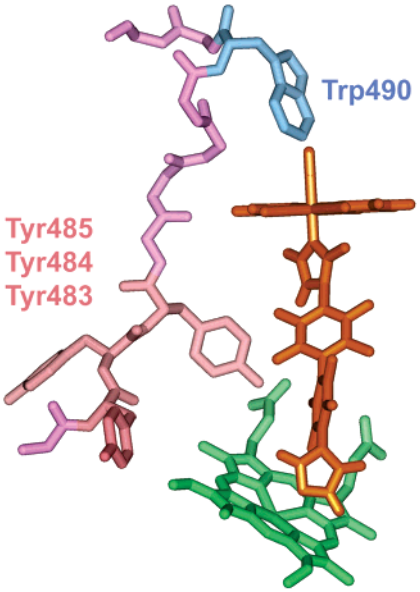

Figure 8. Cutaway view of the model in Figure 7, highlighting the putative tryptophan quencher and three tyrosine residues that could be involved at some stage of the redox chemistry.

lined in Scheme 3. In the case of each wire bound to the protein, excitation at 355 nm produces Re(I)*. Owing to its short length or other binding constraints, excited wire **3** is quenched by Förster energy transfer in approximately 30 ns. The other three bound, photoexcited wires are quenched in less than 200 ps by electron transfer that generates "Re(0)" and a tryptophan radical cation. Recombination in this charge-separated state is likely to occur rapidly. In the case of wire **4**, in which no through-bond pathway to the heme exists, it can be assumed that thermal recombination is the dominant pathway back to the resting state. In the cases of imidazole-terminated wires **1** and **2**, however, a direct bond to the heme allows for rapid electron transfer in competition with recombination, thereby producing Fe(II) within a few hundred picoseconds after excitation. The reduced heme then reacts with oxidized amino acids by multiple pathways over a period of a few hundred microseconds.

In the kinetics model shown in Scheme 3, it is expected that $k_r > k_{ET}$, and that k_r therefore dominates the rate of formation of Fe(II). Thus, an estimate of k_{ET} can be extracted from the data using eq 8 (see the Experimental Section). Measurement of the rate of formation ($k_f = 7(3) \times 10^9$ s^{-1}) and quantum yield (8(2)%) of Fe(II) in the reaction allows us to estimate $k_{ET} \approx 6 \times 10^8$ s^{-1} for the **1**:iNOSoxy conjugate. Even for activationless ET in a conjugated donor−bridge−acceptor system, this rate is too high to be accounted for by single-step tunneling over a distance ≥18 Å.[27] Our tentative proposal is that the ultrafast reduction involves electron hopping through the perfluorobiphenyl bridge or possibly through a tyrosine near the heme (see Figure 8). Simulations based on the Scheme 3 kinetics model that include reasonable estimates of driving forces and reorganization energies indicate that two-step hopping could account for the observed rate (Supporting Information).

Concluding Remarks

We have designed and constructed four Re(I)−diimine wires that bind to the oxidase domain of inducible NOS. Upon photoexcitation, two of these wires are capable of reducing the enzyme almost 10 orders of magnitude faster than naturally occurring electron transfer from the reductase module. The demonstration of photoinduced, subnanosecond production of Fe(II) represents an important step toward the unraveling of the catalytic mechanism of NOS through wire-based technology. Being able to trigger rapid heme reduction in the absence of exogenous quenchers could lead to X-ray structural characterization of high-valent, catalytic intermediates in crystals of enzyme:wire conjugates.

Experimental Section

Syntheses. Dimethyl sulfoxide (DMSO) was purchased from EM Science and dried over calcium hydride. Anhydrous, inhibitor-free tetrahydrofuran (THF) was purchased from Aldrich and used without further purification. All other solvents were either "OmniSolv" grade reagents from EM Science or Burdick and Jackson High Purity solvents and were used as received. Rhenium(I) pentacarbonyl chloride, silver tetrafluoroborate, and silver trifluoromethane sulfonate were purchased from Strem Chemicals. All other reagents were purchased from either Aldrich or EM Sciences. All reagents were used as received. Preparative chromatography on the wire complexes was performed using silica gel (40 μm, 60 Å pore diameter) from JT Baker.

Electrospray ionization mass spectrometry (ESI/MS) was performed on a Finnigan LCQ ion trap mass spectrometer. ^{1}H and ^{19}F NMR spectra were recorded in CD_2Cl_2 on a Varian Mercury 300-MHz spectrometer. The chemical shifts are reported relative to TMS for ^{1}H NMR. ^{19}F NMR spectra were taken without a standard and were used solely for verification of number of fluorine-containing species. Their quoted chemical shifts are, therefore, qualitative.

(4,7-dmp)Re(CO)$_3$Cl. $Re(CO)_5Cl$ (1.0 g, 2.8 mmol) and 4,7-dimethyl-1,10-phenanthroline (4,7-dmp) (0.63 g, 3.0 mmol) were suspended in 50 mL of toluene and stirred at 60 °C overnight. The suspension was removed from heat, filtered, and washed with toluene to obtain a bright yellow solid (1.436 g, 2.8 mmol, 100% yield) which was used without further purification. ^{1}H NMR, $CDCl_3$ (ppm): 2.9 (s, 6H); 7.7 (d, 2H); 8.2 (s, 2H); 9.2 (d, 2H).

[(4,7-dmp)Re(CO)$_3$(OH$_2$)][BF$_4$] (5). (4,7-dmp)$Re(CO)_3Cl$ (0.500 g, 0.98 mmol) was weighed into a sealed, 50-mL, three-neck round-bottom flask and purged with argon for 30 min. Thirty milliliters of anhydrous THF was added, the yellow suspension were stirred for 15 min, and 0.9 equiv of silver tetrafluoroborate (171 mg, 0.88 mmol) was

Scheme 3. Proposed Quenching and ET Processes in Photoexcited Re−Diimine:iNOSoxy Conjugates[a]

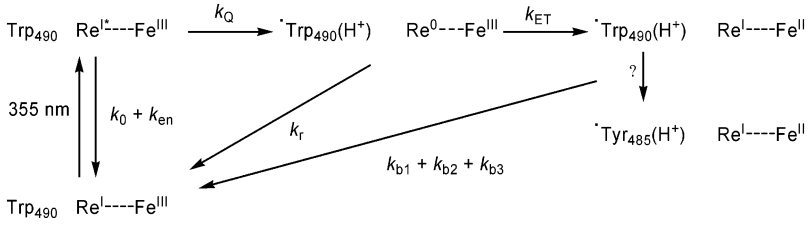

[a] Re(I)* either oxidizes a nearby Trp residue (k_Q) or decays back to the ground state through a combination of Förster transfer (k_{en}) and intrinsic decay (k_0). The transient "Re(0)" species either reduces the heme (k_{ET}) or reacts with the Trp radical (k_r). The charge-separated species produced by this route then decays back to the ground state through multiple pathways (k_{b1}, k_{b2}, k_{b3}).

transferred into the flask under argon flow. The reaction was sealed and left to stir for 24 h. The suspension was then filtered over Celite and rinsed with dry THF to remove silver chloride and obtain a bright yellow solution. The solution was rotary evaporated to dryness to obtain a yellow solid (theoretical yield: 0.88 mmol) that was used without further purification. ^{1}H NMR, CD_3CN (ppm): 3.0 (s, 6H); 7.9 (d, 2H); 8.4 (s, 2H); 9.2 (d, 2H). ^{19}F NMR, CD_3CN (ppm): −152.2 (4F).

Im-F$_9$bp (6) and Im-F$_8$bp-Im (7). Potassium carbonate (1.24 g, 9 mmol) was added to a vacuum-dried 100-mL Schlenk flask under argon flow and dried under heat and vacuum for 1 h. The heat was removed, and imidazole (0.61 g, 9 mmol) was added to the flask under argon flow. The flask was then returned to vacuum for 30 min, and then ∼50 mL of dry DMSO were vacuum-distilled into the flask. Decafluorobiphenyl (2.0 g, 6 mmol) was added to the suspension under argon flow. The reaction was then sealed under argon and stirred for 12 h at 30 °C. The reaction was removed from heat and stirring, and 100 mL of water were added. The resulting mixture was extracted with dichloromethane (3 × 100 mL). The combined organic layer was washed with a further 100 mL of water to remove traces of DMSO. The organic layer was then dried over magnesium sulfate, filtered, and rotary evaporated to a light yellowish oil. The oil was redissolved in minimal dichloromethane and flash chromatographed over silica gel (2:1 ethyl acetate:hexanes). Three organic fractions were collected and rotary evaporated to dryness. The first fraction contained unreacted decafluorobiphenyl. The second contained product **6** as a white solid (0.461 g, 1.2 mmol, 20% yield). ^{1}H NMR, CD_2Cl_2 (ppm): 7.30 (s, 1H); 7.35 (s, 1H); 7.84 (s, 1H). ^{19}F NMR, CD_2Cl_2 (ppm): −161.2 (2F); −150.5 (1F); −148.2 (2F); −138.0 (2F); −137.3 (2F). The third fraction contained product **7** as a white solid (1.243 g, 2.9 mmol, 48% yield). ESI/MS $(m/z)^+$: 431.3 (calcd 431.3). ^{1}H NMR, CD_2Cl_2 (ppm): 7.30 (s, 2H); 7.35 (s, 2H); 7.90 (s, 2H). ^{19}F NMR, CD_2Cl_2 (ppm): −148.0 (4F); −136.9 (4F).

[(4,7-dmp)Re(CO)$_3$(Im-F$_9$bp)][BF$_4$] (3). Product **5** was dissolved in a mixture of 12 mL of dichloromethane and 5 mL of THF and added to **6** (0.342 g, 0.88 mmol). The reaction was stirred at 30 °C. Aliquots were tested by ESI/MS at various time points, and the reaction was removed from heating when the product peak stopped growing (48−120 h). The reaction was then rotary evaporated to an orange oil. The oil was redissolved in minimal dichloromethane and flash chromatographed over silica gel under the following conditions: 3% methanol in dichloromethane until the first two bands (one fluorescent orange band containing various rhenium species and one colorless band containing free **6**) were collected. The methanol was then gradually increased to 40%. The fluorescent yellow-green product was collected and rotary evaporated to dryness to yield a yellow solid (0.122 g, 0.128 mmol, 14.5% yield). ESI/MS $(m/z)^+$: 860.8 (calcd 861). ^{1}H NMR, CD_2Cl_2 (ppm): 3.0 (s, 6H); 6.8 (s, 1H); 7.1 (s, 1H); 7.9 (s, d, 3H); 8.3 (s, 2H); 9.35 (d, 2H). ^{19}F NMR, CD_2Cl_2 (ppm): −161.1 (2F); −152.2 (4F) (BF_4); −150.2 (1F); −148.0 (2F); −137.6 (2F); −136.4 (2F).

[(4,7-dmp)Re(CO)$_3$(Im-F$_8$bp-Im)] [BF$_4$] (1). 7 (0.379 g, 0.88 mmol) was added to a 100-mL, three-neck round-bottom flask fitted with a stir bar and condenser. **5** (0.44 mmol by theoretical yield, 0.5 equiv to prevent bis-Re-substituted wire formation) was dissolved in a mixture of dichloromethane and THF added to the flask. The reaction was stirred at 30 °C until ESI/MS showed that the product peak had stopped growing (2−5 days). The reaction was removed from heat and stirring, and the product was then extracted into dichloromethane and washed with water. The organic solution was dried over magnesium sulfate and rotary evaporated to dryness. The product was redissolved in dichloromethane and flash chromatographed under the same conditions as **3**. The clean product was rotary evaporated to dryness to obtain a yellow solid (0.0807 g, 0.076 mmol, 17.3% yield based on Re concentration). ESI/MS $(m/z)^+$: 908.7 (calcd 909). ^{1}H NMR, CD_2Cl_2 (ppm): 3.0 (s, 6H); 6.8 (s, 1H); 7.1 (s, 1H); 7.25 (s, 1H); 7.35 (s, 1H); 7.8 (s, 1H); 7.9 (d, 2H); 7.95 (s, 1H); 8.3 (s, 2H); 9.4 (d, 2H). ^{19}F NMR, CD_2Cl_2 (ppm): −152.2 (4F) (BF_4); −147.9 (4F); −136.3 (4F).

Im-C$_3$-F$_9$bp (8). Decafluorobiphenyl (3 g, 9.22 mmol) and K_2CO_3 (2.3 g, 16.76 mmol) were stirred in anhydrous DMF (15 mL) under argon. Aminopropylimidazole (1 mL, 8.38 mmol) was added via syringe, and the mixture was stirred overnight at room temperature. Precipitated KF was removed by vacuum filtration through Celite. Water was added to the filtrate, and the product was extracted with dichloromethane (3 × 10 mL). Organic layers were combined, dried over magnesium sulfate, and concentrated. The product was purified by column chromatography on silica gel (CH_2Cl_2:MeOH = 50:1) to obtain a light brown oil (2.2 g, 5.01 mmol, 59.7% yield). ^{1}H NMR, $CDCl_3$ (ppm): 2.2 (m, 2H); 3.5 (t, 2H); 4.3 (t, 2H); 4.7 (s, 1H); 7.0 (s, 1H); 7.2 (s, 1H); 8.65 (s, 1H). ^{19}F NMR, $CDCl_3$ (ppm): −161.8 (2F); −160.2 (2F); −152.4 (1F); −141.0 (2F); −138.2 (2F).

[(4,7-dmp)Re(CO)$_3$(Im-C$_3$-F$_9$bp)][BF$_4$] (4). 5 (1 g, 1.71 mmol) and **8** (0.75 g, 1.71 mmol) were stirred in a 2:1 mixture of CH_2Cl_2:THF (5 mL) at 40 °C for 5 days. The reaction mixture was cooled to room temperature, filtered through Celite, and washed with CH_2Cl_2. The filtrate was concentrated and flash chromatographed over silica gel (CH_2Cl_2:MeOH = 50:3). The product fraction was rotary evaporated to dryness to obtain a bright yellow solid (900 mg, 0.89 mmol, 52.2% yield). ESI/MS $(m/z)^+$: 917.9 (calcd 918.1). ^{1}H NMR, CD_2Cl_2 (ppm): 1.95 (m, 2H); 3.0 (s, 6H); 3.3 (t, 2H); 3.9 (t, 2H); 4.6 (s, 1H); 6.5 (s, 1H); 6.8 (s, 1H); 7.25 (s, 1H); 7.9 (d, 2H); 8.3 (s, 2H); 9.3 (d, 2H). ^{19}F NMR, DMSO (ppm): −161.8 (2F); −160.8 (2F); −152.2 (1F); −148.6 (4F) (BF_4); −142.4 (2F); −139.4 (2F).

[(4,7-dmp)Re(CO)$_3$(Im-C$_3$-F$_8$bp-Im)][BF$_4$] (2). Imidazole (74.3 mg, 1.09 mmol) and K_2CO_3 (150 mg, 1.09 mmol) were stirred in anhydrous DMF (5 mL). **4** (1 g, 0.99 mmol) was added, and the reaction was stirred under argon overnight at room temperature. The reaction mixture was then filtered through Celite and washed with CH_2Cl_2. The filtrate was concentrated and flash chromatographed over silica gel (CH_2Cl_2:MeOH = 50:3). The product fraction was rotary evaporated to dryness to obtain a bright yellow solid (700 mg, 0.66 mmol, 67% yield). ESI/MS $(m/z)^+$: 965.1 (calcd 966.1). ^{1}H NMR, CD_2Cl_2 (ppm): 1.95 (m, 2H); 3.0 (s, 6H); 3.3 (t, 2H); 3.9 (t, 2H); 4.6 (s, 1H); 6.5 (s, 1H); 6.8 (s, 1H); 7.25 (s, 1H); 7.3 (s, 1H); 7.35 (s, 1H); 7.8 (s, 1H); 7.9 (d, 2H); 8.3 (s, 2H); 9.3 (d, 2H). ^{19}F NMR, CD_2Cl_2 (ppm): −161.2 (2F); −152.2 (4F) (BF_4); −149.4 (2F); −142.2 (2F); −137.8 (2F).

Sample Preparation. Δ65 iNOSoxy samples were prepared as described previously.[35] Small aliquots of the protein solutions were exchanged into phosphate buffer (50 mM potassium phosphate, 50 mM potassium chloride, pH 7.4) ("buffer") using a desalting column immediately before use. The measurement of the heme Soret maximum at 422 nm confirmed the presence of low-spin, water-bound heme. Monomeric, heme-containing protein concentration was determined using the extinction coefficient $\epsilon_{422} = 75\ mM^{-1}\ cm^{-1}$.[19]

Due to their low solubilities in water (∼20 μM for **1** and **3** and ≤1 μM for **2** and **4**), concentrated (0.5−1.5 mM) wire solutions were prepared in absolute ethanol. Small aliquots were then added to buffer/protein samples such that the overall ethanol concentration never exceeded 2%.[36] Repeated experiments indicated a large degree of error in measured concentration by this method. As the measured concentration was consistently lower than expected, the error is likely due to the affinity of the hydrophobic wires for either glass syringes or plastic pipet tips. As such, protein:wire samples for rigorous quantitation were prepared by adding wire solutions to buffer, measuring the concentration by UV−visible absorption, and then adding a known quantity of protein.

Samples of **2** and **4** for rigorous quantitative characterization were prepared in 50% glycerol in buffer. Attempts were made to conduct protein:wire studies in this type of mixture, but both glycerol and ethylene glycol blue-shifted the heme Soret, indicating that they were binding to the enzyme. These mixtures also interfered with wire binding,

(35) Ghosh, D. K.; Wu, C. Q.; Pitters, E.; Moloney, M.; Werner, E. R.; Mayer, B.; Stuehr, D. J. *Biochemistry* **1997**, *36*, 10609−10619.
(36) Testing with Δ65 indicated that micromolar protein solutions could tolerate 5% ethanol with no spectroscopic evidence of heme loss or preciptation.

supporting the hypothesis that hydrophobic burial of the perfluorobiphenyl unit provides a good deal of binding energy to the wire:protein conjugates.

UV−visible absorption spectra were taken on an Agilent 8453 UV spectrometer. Steady-state emission measurements were made in buffer using a Flurolog model FL3-11 fluorometer equipped with a Hamamatsu R928 photomultiplier tube. Emission quantum yields (ϕ) were determined in deoxygenated solutions relative to tris(2,2′-bipyridine)ruthenium(II) ($\phi = 0.042$ in water).[37] All steady-state emission and transient spectroscopic measurements were made in sealed quartz cuvettes with deoxygenated samples (at least 30 cycles of partial evacuation followed by backfilling with argon) unless otherwise stated.

Transient Spectroscopy. Nanosecond luminescence decay and transient absorption measurements were made using a frequency-tripled Nd:YAG laser ($\lambda = 355$ nm) as the excitation source in an apparatus that has been described elsewhere.[38,39] The instrument has a response limit of approximately 10 ns. Luminescence decay curves for the wires and Δ65:wire complexes were fit in Igor Pro using a nonlinear least-squares algorithm according to the following expression (eq 1):

$$I(t) = c_0 + \sum_n c_n \, e^{-k_n t} \tag{1}$$

where $n = 1-3$ for mono-, bi-, and triexponential decays, respectively. Transient absorbance data were converted from intensity to optical density using eq 2:

$$\mathrm{OD} = -\log(I/I_0) \tag{2}$$

where I is the intensity of transmitted light after excitation and I_0 was taken as the average light intensity over the 200 ns prior to the laser shot. Decays of the Fe(II) signals observed upon photoreduction of the enzyme were fit using eq 1. The quantum yield of Fe(II) was calculated at $t = 20$ ns using the following expression (eq 3):

$$[\mathrm{Fe(II)}] = \Delta \mathrm{OD}_{445}/\Delta\epsilon_{445} \tag{3}$$

where $\Delta\epsilon_{445}$ (six-coordinate Fe(III) − six-coordinate Fe(II)) was estimated by subtracting the absorptivity measured for wire-bound ferric Δ65 iNOSoxy from the absorptivity reported for six-coordinate ferrous iNOSoxy (105.4 $\mathrm{mM^{-1}\,cm^{-1}}$).[40] For these measurements, an excess of protein was included in the sample in order to minimize contributions to the transient absorbance signal from free Re(I)*, and sufficient laser power was used to ensure that 100% of the wire in the sample was excited.

For picosecond transient absorption measurements, the samples were excited at 10 Hz with 70-ps, 355-nm pulses from a regeneratively amplified, mode-locked Nd:YAG laser. To eliminate interference from fluorescence either of free wire or protein, the sample was placed far from the detector and probed with 442-nm light from a continuous-wave HeCd laser. Stray light from the room was filtered with a 442-nm notch filter, and light intensity with (I, 10 000 counts) and without (I_0, 10 000 counts) excitation of the sample was collected directly by a fiber optic (Fiberguide Industries) and detected with a Hamamatsu C5680 streak camera. The raw image files were converted to *xy* data using an in-house macro for Matlab. The raw data were then converted to optical density using eq 2, and the rate of formation of ferrous heme was fit to one exponential using eq 1.

Because the resting (ferric) heme already has appreciable absorbance at 442 nm, the initial probe light intensity, and therefore the overall signal strength, was attenuated. Additionally, the protein would not tolerate more than about 20 000 pump/probe shots before it began to visibly deteriorate by precipitating from solution. A compromise between sample concentration, probe laser power, and total laser shots was therefore made in order to maximize signal-to-noise ratio.

Dissociation Constants. In the case of the Δ65:**3** complex, the equilibrium dissociation constant was calculated from the biexponential fit of the luminescence decay (eq 1, $n = 2$) as described previously.[21] Due to the rapidity of the luminescence decay of bound wire **1**, the Δ65:**1** dissociation constant was calculated as described in earlier work from steady-state luminescence spectra.[19] Because of their low solubilities and tendency to aggregate in water, dissociation constants for **2** and **4** with Δ65 could not be reproducibly determined. In approximately 1:1 wire:protein mixtures at 1−10 μM concentrations, however, observation of significant Δ65 heme Soret shifts and visible luminescence quenching of the wires allowed for the estimation of micromolar dissociation constants for both wires.

Förster Energy Transfer. Förster energy transfer (FET) parameters were obtained from eq 4:

$$k_{\mathrm{en}} = k_0(R_0/R)^6 \tag{4}$$

where k_0 is the intrinsic luminescence decay rate of the donor (the rhenium sensitizer), R is the distance between donor and acceptor (the iNOS heme group), and R_0, the Förster distance, is the distance at which half of the luminescence intensity of the donor is quenched by FET. R_0 was calculated (in cm) from eq 5:

$$R_0{}^6 = 8.8 \times 10^{-25}(\kappa^2 n^{-4} \phi_{\mathrm{D}} J) \tag{5}$$

where the overlap integral $J = \int F_{\mathrm{D}}(\lambda)\, \epsilon_{\mathrm{A}}(\lambda)\, \lambda^4\, \mathrm{d}\lambda$, κ^2 is a measure of the spatial orientation of the transition dipoles of the donor and acceptor with respect to each other ($\kappa^2 = 2/3$ in randomly oriented pairs), n is the refractive index of the solvent ($n = 1.34$ for water), and ϕ_{D} is the luminescence quantum yield of the donor.[24]

Estimation of ET Rate Constants. The kinetics for luminescence quenching and electron transfer in this system were interpreted according to the model in Scheme 3. The observed rate constant (k_{L}) for the decay of Re(I)* in the presence of iNOSoxy is

$$k_{\mathrm{L}} = k_0 + k_{\mathrm{en}} + k_{\mathrm{Q}} \tag{6}$$

The rate of Fe(II) formation depends on the concentration of "Re(0)", so the observed rate constant (k_{f}) is given by

$$k_{\mathrm{f}} = k_{\mathrm{r}} + k_{\mathrm{ET}} \tag{7}$$

Because k_{r} describes a nonproductive reaction, k_{ET} can be extracted from k_{f} through the following expression:

$$\Phi_{\mathrm{ET}} = k_{\mathrm{ET}}/(k_{\mathrm{ET}} + k_{\mathrm{r}}) = k_{\mathrm{ET}}/k_{\mathrm{f}} \tag{8}$$

where Φ_{ET} is the quantum yield of Fe(II) as a percentage of Re(I)* in the wire-bound sample assuming $k_{\mathrm{Q}} \gg k_0 + k_{\mathrm{en}}$.

Acknowledgment. This research was supported by NIH (DK19038; GM070868), the Parsons Foundation (W.B.-B.), the Fannie and John Hertz Foundation (A.R.D.), the Ellison Medical Foundation (Senior Scholar Award in Aging to H.B.G.), and the Arnold and Mabel Beckman Foundation.

Supporting Information Available: Semilog plots with fits of the luminescence decay data for the **2**:Δ65 and **4**:Δ65 complexes; single-wavelength transient absorbance data for the **1**:Δ65 complex; kinetics simulation for electron hopping. This material is available free of charge via the Internet at http://pubs.acs.org.

JA0543088

(37) Van Houten, J.; Watts, R. J. *J. Am. Chem. Soc.* **1976**, *98*, 4853−4858.
(38) Low, D. W.; Winkler, J. R.; Gray, H. B. *J. Am. Chem. Soc.* **1996**, *118*, 117−120.
(39) Dmochowski, I. J.; Winkler, J. R.; Gray, H. B. *J. Inorg. Biochem.* **2000**, *81*, 221−228.
(40) Hurshman, A. R.; Marletta, M. A. *Biochemistry* **2002**, *41*, 3439−3456.